PHYSICAL REVIEW C VOLUME 25, NUMBER 3 MARCH 1982

High-spin states in neutron-deficient nuclei near $A=80$

L. V. Theisen,* S. L. Tabor, L. R. Medsker,† G. Neuschaefer, L. H. Fry, Jr., and J. S. Clements
Department of Physics, Florida State University, Tallahassee, Florida 32306
(Received 13 August 1981)

In-beam γ-ray spectroscopy with the reactions $^{54}Fe + {}^{28}Si$ and $^{56}Fe + {}^{28}Si$ at beam energies from 80 to 99 MeV were used to study high-spin states in neutron-deficient nuclei in the mass $A \sim 80$ region. Measurements of γ-ray energies, intensities, angular distributions, excitation functions, and γ-γ coincidences were used to assign new levels in ^{79}Rb and ^{80}Sr. For the first time, high-spin states in ^{81}Sr have been observed.

[NUCLEAR REACTIONS $^{56}Fe(^{28}Si,xpyn\gamma)$ and $^{54}Fe(^{28}Si,xpyn\gamma)$ $E_{lab}=80-99$ MeV; measured E_γ, I_γ, γ-γ coincidences, $\sigma(E_\gamma,E)$, and $\sigma(E_\gamma,\theta)$; ^{79}Rb, ^{80}Sr, and ^{81}Sr deduced levels, J^π. Enriched targets.]

I. INTRODUCTION

The present work is part of a continuing program utilizing ^{28}Si beams to study high-spin states via in-beam γ-ray spectroscopy.[1,2] Heavy-ion-induced fusion reactions are particularly useful for studying high-spin states because of the large amount of angular momentum which they bring into the compound nucleus. Since ^{28}Si does not have a neutron excess it is useful for studying neutron-deficient nuclei in the mass $A \sim 80$ region.

The neutron-deficient isotopes of Kr, Rb, Sr, Y, and Zr lie in a transitional region from closed shell nuclei (near $N=50$; $Z=38$ and 40) to deformed nuclei near $N \sim 40$. Therefore the structure of these nuclei tends to be more complicated, which makes theoretical analyses difficult. Because of the complexity, detailed and systematic studies are important for an understanding of the nuclear structure in this mass region. In addition little is known about the most neutron-deficient Sr, Y, and Zr isotopes, so systematic studies are needed to facilitate the identification of new nuclear level schemes in previously unobserved nuclei. This work will concentrate on the most neutron-deficient Sr nuclei.

II. EXPERIMENTAL PROCEDURE

An inverted sputter source[3] was used to produce beams of ^{28}Si which were accelerated by the Florida State University Super-FN tandem Van de Graaff accelerator. ^{28}Si beams of 80–99 MeV with beam currents of 10–30 nA were used on target. All experiments were carried out using either ^{54}Fe or ^{56}Fe targets. The $^{54}Fe + {}^{28}Si$ γ-γ coincidence experiment used a rolled foil enriched to 99.66% in ^{54}Fe with a thickness of 3.00 mg/cm^2. All other experiments with this reaction used a 100 μg/cm^2 target enriched to 92.47% in ^{54}Fe and evaporated onto a 0.53 mm thick tantalum backing. All experiments with the $^{56}Fe + {}^{28}Si$ reaction were performed using a 400 μg/cm^2 thick target enriched to 99.8% in ^{56}Fe and evaporated onto a 0.53 mm thick tantalum backing.

The γ rays were detected with lithium-drifted germanium [Ge(Li)] detectors. The detectors used were large volume closed-ended coaxial detectors made by Princeton Gamma Tech (PGT) and Ortec. The PGT detector has an 18.6% efficiency at 25 cm source-to-detector distance, relative to a 7.6×7.6 cm NaI(Tl) detector. This detector has an energy resolution of 1.97 keV full width at half maximum (FWHM) at 1.33 MeV. The Ortec detector has a 27% relative efficiency and an energy resolution of 1.95 keV FWHM. Efficiency and energy calibrations were obtained using a National Bureau of Standards (NBS) (Ref. 4) mixed radio-nuclide source. The source was placed at the target location inside the scattering chamber for calibrations. Internal energy calibrations were also obtained using γ rays produced from ^{16}O and ^{12}O contaminants.

Singles γ spectra were measured at an angle of

 ©1982 The American Physical Society

90° to the beam axis. These measurements were used to obtain accurate values for the energies and intensities of γ rays, as a first step in deducing level schemes. The singles spectra were analyzed using a modified version of the computer code PEAKFIT.[5] The program performs a least squares fit of Gaussian distributions to the peaks in a spectrum, by varying the FWHM, height, and background parameters of the Gaussian curves in an iterative procedure. An example of a singles spectrum is shown in Fig. 1. The results of the singles experiments are given in Tables I and II. Beam-off spectra were taken immediately following bombardment, to help identify reaction products.

Excitation functions, measurements of intensity as a function of beam energy, were taken over the laboratory energy range of 80–99 MeV in 5 MeV steps. This energy step size was chosen because the energy loss in the targets was on the order of 2 MeV. Normalization between beam energies was obtained by using the total accumulated beam charge. Excitation functions are useful in γ-ray spectroscopy, since γ rays from the same residual nucleus should have excitation functions of relatively similar shape. As the beam energy is increased more angular momentum and energy are brought into the reaction and states with higher angular momentum become populated. Therefore, γ rays depopulating higher spin states should have greater intensities, relative to the next lower transition, at higher energies. This gives evidence for the assignment of γ rays to higher or lower spin states depending on the slope of the excitation functions. That is γ rays originating in higher spin states will have greater slopes relative to those originating from lower spin states.

Angular distributions for γ rays are symmetric about 90° to the beam axis, because of parity conservation. Therefore, measurements of angular distributions were made over the angular range 0 to 90°. Measurements were made at five angles in this range in equal increments of $\cos^2\theta$. The normalization between angles was obtained by using the total accumulated charge at each angle. A second detector placed at $-90°$ to the beam was used as a monitor and a check on the normalization between angles. A computer program ANGDIS[6] was used to obtain a least squares fit of the equation

$$I(\theta)=A_0[\,1+A_2/A_0P_2(\cos\theta) + A_4/A_0P_4(\cos\theta)]\,,$$

to the angular distribution data. $I(\theta)$ is the intensity at angle θ and P_2 and P_4 are Legendre polynomials of order 2 and 4, respectively. A_0, A_2, and A_4 are parameters obtained from the least squares fit to the data. The program weights the data points according to their uncertainties. The values A_2/A_0 and A_4/A_0 and their respective errors are calculated by the program, as well as a fit to the data. Only Lengendre polynomials of order 2 and 4 are used for the fits for the following reasons: First, all odd terms in the Legendre polynomial expansion cancel,

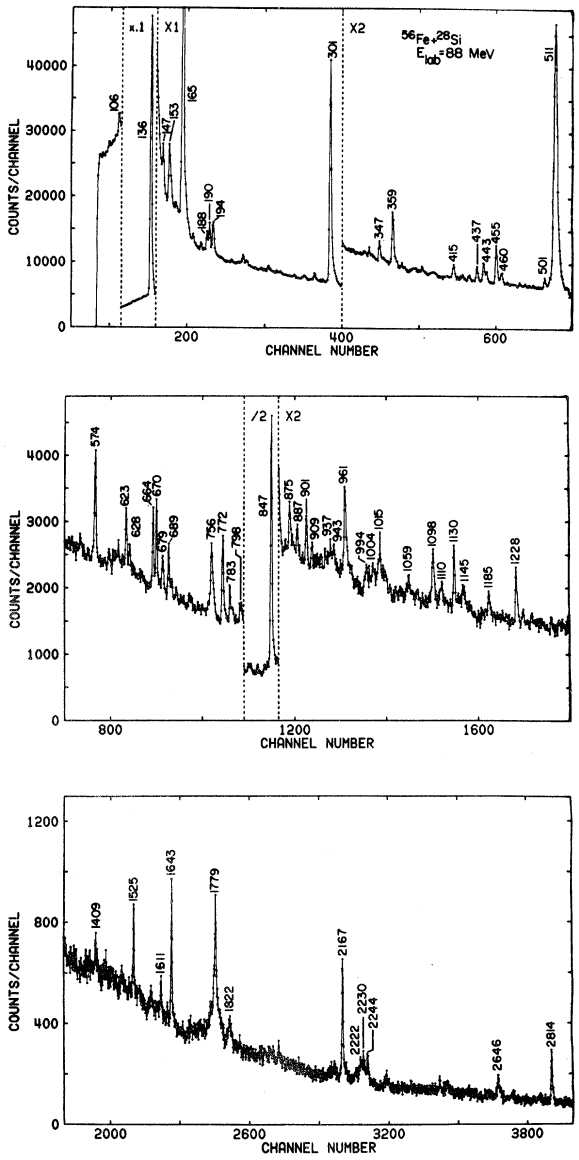

FIG. 1. An example of a γ ray singles spectrum from the reaction $^{56}\mathrm{Fe}+{}^{28}\mathrm{Si}$ at $E_{\mathrm{lab}}=88$ MeV. The energies of the γ rays shown above the peaks are in keV.

TABLE I. Results from the singles experiment for the reaction $^{54}Fe + ^{28}Sr$ at $E_{lab}=90$ MeV.

E_γ (keV)[a]	$(I_\gamma \times 10^{-6})$[b]	Assign	E_γ^{lit} (keV)±error
105.8	37	^{38}Ar	105.3 ±0.3[d]
		^{79}Rb	104.99±0.08[i]
129.7	21	^{79}Kr	129.72±0.01[h]
		^{181}Ta	136.25±0.02[c]
136.3	3170	^{76}Br	134.8 ±0.2[j]
152.3	34		
154.5	20	^{79}Kr	154.82±0.01[h]
160.0	46	^{79}Kr	160.76±0.01[h]
165.2	560	^{181}Ta	165.2 ±0.2[c]
167.9	211	^{41}Ca	168.34±0.10[f]
177.2	30		
182.7	35	^{79}Kr	182.77±0.01[h]
193.7	39	^{181}Ta	193.8 ±0.3[c]
218.9	24	^{79}Kr	218.8 ±0.4[h]
			219.3 ±0.4[h]
221.6	39	^{181}Ta	221.5 ±0.3[c]
246.5	21	^{41}K	246.48±0.10[f]
251.7	11	^{39}K	251.9 ±0.40[e]
		^{76}Br	252.1 ±0.2[j]
261.1	14		
264.2	14	^{42}Ca	263.8 ±0.4[g]
267.7	10		
270.2	21	^{76}Br	270.3 ±0.2[j]
279.3	6	^{77}Kr	279.0 ±0.4[n]
301.5	450	^{181}Ta	301.3 ±0.3[c]
315.8	19	^{76}Br	315.7 ±0.2[j]
323.7	13		
333.1	9		
346.6	98	^{39}K	346.8 ±0.4[e]
350.8	32	^{79}Kr	350.6 ±0.01[h]
359.0	56	^{181}Ta	358.8 ±0.3[c]
378.1	7		
382.1	20		
385.9	34	^{80}Sr	385.4 ±0.3[m]
397.8	22	^{79}Kr	397.6 ±0.1[h]
406.3	8	^{76}Br	406.5 ±0.2[j]
415.1	37	^{181}Ta	415.1 ±0.3[c]
423.9	43	^{76}Kr	423.8[j]
437.1	120	^{42}Ca	437.04±0.18[g]
454.9	19	^{78}Kr	455.3 ±0.3[k]
460.4	82	^{41}Ca	460.12±0.10[f]
497.0	12		
501.1	78	^{79}Rb	501.2 ±0.5[l]
505.6	55	^{79}Kr	505.4 ±0.1[h]
511.3	1090	e^+-e^-	511.00
533.4	6		
546.0	18	^{41}Ca	545.1 ±0.3[f]
553.2	3	^{76}Br	552.6 ±0.3[j]

TABLE I. (*Continued.*)

E_γ (keV)[a]	$(I_\gamma \times 10^{-6})$[b]	Assign	E_γ^{lit} (keV)±error
559.3	23		
584.6	2		
589.4	19		
595.5	42	^{80}Sr	594.8 ±0.3[m]
601.2	7		
606.2	11		
610.8	40	^{76}Kr	610.4[j]
616.7	13		
622.5	19	^{79}Kr	622.2 ±0.1[h]
657.6	4		
664.8	14	^{78}Kr	664.8 ±0.5[k]
670.0	106	^{38}Ar	669.86±0.15[d]
680.3	15		
688.7	57	^{79}Kr	688.1 ±0.1[h]
708.5	10	^{41}K	708.25±0.10[f]
756.9	147	^{79}Rb	755.6 ±0.5[l]
		^{39}K	757.2 ±0.4[e]
771.6	13		
774.8	21	^{38}Ar	775.1 ±0.3[d]
783.6	80	^{39}K	783.4 ±0.4[e]
		^{80}Sr	783±0.5[m]
810.1	48	^{42}Ca	809.8 ±0.4[g]
815.2	53	^{42}Ca	814.8 ±0.4[g]
824.9	17	^{76}Kr	824.8[j]
846.9	13		
850.6	14	^{41}K	850.34±0.15[f]
875.5	10		
887.1	70	^{39}K	886.9 ±0.4[e]
892.6	7		
910.8	17	^{42}Ca	910.5 ±0.4[g]
918.1	20	^{42}Ca	917.8 ±0.4[g]
923.9	11		
929.6	17	^{42}Ca	929.1 ±0.5[g]
937.2	13	^{80}Sr	
946.5	11		
962.4	24	^{79}Rb	962.7 ±0.5[l]
993.5	14		
1014.5	9	^{27}Al	1014.4 ±0.5[o]
1018.9	8	^{76}Kr	1017[j]
1065.1	8	^{80}Sr	
1098.5	7		
1130.5	156	^{39}K	1130.2 ±0.4[e]
1144.9	10	^{79}Rb	
1185.6	21	^{80}Sr	
1228.2	152	^{42}Ca	1227.66±0.14[g]
1294.0	23	^{41}K	1293.64±0.04[f]
1301.7	21	^{39}K	1301.3 ±0.4[e]
1342.4	19		
1347.8	14	^{42}Ca	1347.4 ±0.2[g]
1398.9	30	^{41}Ca	1389.2 ±0.4[f]
1409.0	104	^{39}K	1410.1 ±0.5[e]

TABLE I. (*Continued.*)

E_γ (keV)[a]	$(I_\gamma \times 10^{-6})$[b]	Assign	E_γ^{lit} (keV)± error
1468.8	17	^{41}K	1468.2 ±0.2[f]
1500.8	6	^{41}K	1500.1 ±0.2[f]
1513.2	10	^{41}K	1512.8 ±0.2[f]
1525.1	175	^{42}Ca	1524.58±0.08[g]
1607.5	15		
1643.1	127	^{38}Ar	1642.42±0.10[d]
		^{42}Ca	1644.5 ±0.4[g]
1677.7	14	^{41}K	1676.9 ±0.2[f]
1764.7	22		
1774.7	98	^{39}K	1774.2 ±0.2[e]
1779.4	78	^{28}Si	1779.1 ±0.2[o]
1788.3	39		
1792.1	35		
1822.7	13	^{38}Ar	1823.0 ±0.4[d]
1970.6	42		
2167.9	129	^{38}Ar	2167.53±0.05[d]
2177.2	37		
2208.1	30		
2244.0	8		
2302.0	56	^{42}Ca	2301.7 ±0.3[g]
2489.9	29		
2554.8	20	^{42}Ca	2554.8 ±0.3[g]
2576.1	15		
2646.1	15		
2686.8	12		
2690.4	18		
2814.1	223	^{39}K	2813.6 ±0.3[e]
2859.0	8		

[a]Uncertainties in energies are ±0.5 keV.
[b]Uncertainties in intensities vary from 10% for the strongest peaks to 50% for the weakest peaks.
[c]Reference 18.
[d]Reference 19.
[e]Reference 20.
[f]Reference 21.
[g]Reference 22.
[h]Reference 23.
[i]Reference 14.
[j]Reference 24.
[k]Reference 25.
[l]Reference 9.
[m]Reference 12.
[n]Reference 26.
[o]Reference 27.

because the angular distributions are symmetric about 90° to the beam axis. Second, the probability of γ rays being emitted with multipolarities greater than quadrupole is very small, so only the order 2 and 4 are used. It is well known that heavy-ion reactions produce compound nuclei that are highly aligned and the alignment is transferred to the first observed state in the final nucleus. Furthermore

TABLE II. Results of the singles experiment for the reaction $^{56}Fe + {}^{28}Si$ at $E_{lab} = 88$ MeV.

E_γ (keV)[a]	$(I_\gamma \times 10^{-6})$[b]	Assign	E_γ^{lit} (keV) ± error
97.5	0.9	^{81}Rb	98 ± 1[h]
105.8	3.6	^{38}Ar	105.3 ± 0.3[d]
136.3	631	^{181}Ta	136.25 ± 0.02[c]
147.4	6.6	^{81}Rb	147.8 ± 0.3[h]
		^{79}Kr	147.06 ± 0.01[i]
153.4	15.5	^{81}Rb	153.4 ± 0.4[h]
		^{79}Kr	154.82 ± 0.01[i]
159.2	1.4		
165.2	127	^{181}Ta	165.2 ± 0.2[c]
175.2	2.4	$^{71}Ge^m$	175.2 ± 0.1[g]
182.7	1.2	^{79}Kr	182.77 ± 0.01[i]
188.0	4.8	^{81}Rb	188.3 ± 0.3[h]
190.3	7.1	^{81}Kr	190.1 ± 0.3[h]
193.6	10.4	^{181}Ta	193.8 ± 0.3[c]
221.1	3.9	^{181}Ta	221.5 ± 0.3[c]
223.9	1.9		
244.5	1.5	^{81}Kr	244.2 ± 0.3[h]
277.3	2.5		
286.9	3.5	^{79}Kr	286.2 ± 0.1[i]
301.4	90.7	^{181}Ta	301.3 ± 0.3[c]
		^{81}Rb	301.2 ± 0.3[h]
332.8	1.0		
337.2	1.2		
346.7	4.8	^{39}K	346.8 ± 0.4[e]
358.9	13.4	^{181}Ta	358.8 ± 0.3[c]
		^{81}Kr	357.9 ± 0.2[h]
378.6	1.7		
386.0	1.4	^{80}Sr	385.4 ± 0.3[l]
		^{81}Rb	386.5 ± 0.5[h]
395.7	2.0		
415.0	4.5	^{181}Ta	415.1 ± 0.3[c]
423.3	1.5	^{76}Kr	423.8 ± 0.4[l]
429.6	1.6		
436.9	4.3	^{42}Ca	437.04 ± 0.18[f]
443.2	6.4	^{81}Rb	443.5 ± 0.3[h]
446.1	2.8	^{81}Kr	446.3 ± 0.2[h]
454.9	12.2	^{78}Kr	455.3 ± 0.3[j,m]
459.8	5.1		
500.8	3.4	^{79}Rb	501.2 ± 0.5[k]
		^{81}Kr	499.7 ± 1.5[h]
511.1	168	e^+-e^-	511.00
550.6	1.5	^{81}Rb	549.2 ± 0.5[h]
		^{81}Kr	549.2 ± 0.3[h]
573.9	9.9	^{82}Sr	573.4 ± 0.3[l]
		^{81}Rb	574.6 ± 0.3[h]
595.4	1.5	^{80}Sr	594.8 ± 0.3[l]
601.7	1.2	^{82}Sr	602.1[o]
		^{81}Kr	602.0 ± 0.5[h]

TABLE II. (*Continued*).

E_γ (keV)[a]	$(I_\gamma \times 10^{-6})$[b]	Assign	E_γ^{lit} (keV)±error
610.1	1.8	^{74}Ge ^{76}Kr	609.0[g] 610.4 ± 0.4[l]
622.6	5.8	^{81}Rb ^{79}Kr	623[n] 622.1 ± 0.1[i]
627.7	2.3		
664.3	7.8	^{78}Kr	664.8 ± 0.5[j,m]
669.7	8.8	^{38}Ar ^{63}Cu	669.86± 0.15[d] 669[g]
679.3	5.3		
688.6	4.9	^{79}Kr	688.1 ± 0.1[i]
692.8	2.5	^{72}Ge ^{78}Kr	693[g] 692.9 ± 0.3[j]
700.3	1.6	^{81}Rb	701.5 ± 1.0[h]
721.8	1.9	^{81}Rb	721.3 ± 0.3[h]
755.6	11.1	^{82}Sr	755.1 ± 0.5[l]
772.4	10.8	^{79}Rb	755.6 ± 0.5[k]
		^{81}Sr ^{38}Ar	775.1 ± 0.3[d]
783.3	3.6	^{80}Sr ^{39}K	783 ± 0.5[l] 783.4 ± 0.4[e]
786.7	2.0		
798.4	2.1		
801.0	1.7		
804.0	0.7	^{81}Kr	803.4 ± 0.2[h]
810.6	1.9	^{42}Ca	809.8 ± 0.4[f]
814.8	2.5	^{42}Ca	814.8 ± 0.4[f]
825.3	1.8	^{76}Kr	824.8 ± 0.4[l]
836.4	2.2		
840.3	2.4		
846.7	50.7	^{56}Fe	846.69± 0.14[g]
854.9	5.5		
857.9	4.7	^{78}Kr	859.0 ± 0.7[m]
868.0	0.5	^{74}Ge	868.3[g]
875.2	3.2	^{81}Rb	875[n]
879.0	0.9		
886.7	1.7	^{39}K	886.9 ± 0.4[e]
900.9	3.0	^{82}Sr	901.1 ± 0.5[l]
909.4	1.1	^{42}Ca ^{81}Rb	910.5 ± 0.4[f] 909.3 ± 0.3[h]
929.3	1.3	^{42}Ca	929.1 ± 0.5[f]
937.5	2.1	^{81}Rb	938.6 ± 0.3[h]
943.2	2.1		
960.9	9.5	^{81}Sr ^{79}Rb	962.7 ± 0.5[k]
994.2	2.6		
1003.4	2.5		
1013.0	2.7	^{82}Sr	1013.4 [o]

TABLE II. (*Continued.*)

E_γ (keV)[a]	$(I_\gamma \times 10^{-6})$[b]	Assign	E_γ^{lit} (keV)± error
1014.8	3.0	^{78}Kr	1015.0 ± 0.5[n]
		^{27}Al	1014.4 ± 0.2[g]
1023.0	2.1	^{81}Rb	1024[n]
1059.3	2.2		
1072.9	1.1	^{79}Kr	1072.3 ± 0.3[i]
1097.5	5.0	^{81}Sr	
1110.0	2.5	^{82}Sr	1107.6[o]
		^{78}Kr	1109.7 ± 0.3[j]
1130.1	4.8	^{39}K	1130.2 ± 0.4[e]
1144.6	2.4	^{81}Sr	
		^{79}Rb	
1184.6	2.9		
1227.7	5.6	^{42}Ca	1227.66± 0.14[f]
1237.6	1.3		
1251.2	0.9		
1282.5	1.0		
1294.3	1.3		
1300.4	1.1	^{39}K	1301.3 ± 0.5[e]
1309.9	1.4		
1408.1	2.2	^{39}K	1410.1 ± 0.5[e]
1524.6	5.9	^{42}Ca	1524.58± 0.08[f]
1610.6	2.1		
1642.8	10.4	^{38}Ar	1642.42± 0.10[d]
		^{42}Ca	1644.5 ± 0.4[f]
1762.6	1.4		
1774.7	5.6	^{39}K	1774.2 ± 0.4[e]
1779.0	12.6	^{28}Si	1779.1 ± 0.2[g]
1822.5	2.4	^{38}Ar	1823.0 ± 0.4[d]
2167.2	12.3	^{38}Ar	2167.53± 0.05[d]

this type of reaction tends to populate yrast states (i.e., levels of the highest possible angular momentum for a given excitation energy). As a result each successively lower level has a lower spin by one or two units of angular momentum from the preceding level. Therefore, the γ-ray angular distributions can be used to assign multipolarities and spins, since there is little mixing of magnetic substates.[7]

Since there are numerous γ rays in a singles spectrum it is impossible to assign γ rays to a cascade with certainty without doing γ-γ coincidence experiments. These experiments determine the feeding of various levels, and correlate the γ rays seen in a given nucleus. The γ-γ coincidence experiments were performed with the Ge(Li) detectors placed at $\pm 90°$ to the beam axis. The timing resolution of the time-to-amplitude converter (TAC) peak was better then 15 nsec FWHM for both coincidence experiments. The multiparameter data generated in these experiments consisted of three channel numbers corresponding to the two energy signals and a TAC signal. The data was accumulated event-by-event and stored sequentially on magnetic tape by means of a Univac 6130 computer. Using the computer code RAMPS[8] the multiparameter data was sorted on specific peaks or background regions of the energy or TAC spectra. Final gated energy spectra were obtained by subtracting the background spectra from the gated peak spectra. The background spectra were generated by gating on an equal width con-

TABLE II. (*Continued.*)

E_γ (keV)[a]	$(I_\gamma \times 10^{-6})$[b]	Assign	E_γ^{lit} (keV)± error
2221.9	1.8		
2230.8	2.3	$H(n,\gamma)D$	2229[g]
2243.5	2.8		
2302.0	1.1	^{42}Ca	2301.7 ± 0.3[f]
2465.8	1.1		
2646.0	2.9		
2814.1	8.1	^{39}K	2813.6 ± 0.3[e]

[a]Uncertainties in energies are ±0.5 keV.
[b]Uncertaintites in intensities vary from 10% for the strongest peaks to 50% for the weakest peaks.
[c]Reference 18.
[d]Reference 19.
[e]Reference 20.
[f]Reference 22.
[g]Reference 27.
[h]Reference 28.
[i]Reference 23.
[j]Reference 29.
[k]Reference 9.
[l]Reference 12.
[m]Reference 25.
[n]Reference 30.
[o]Reference 31.

tinuum region adjacent to the peak. Accidental coincidences were negligible in these experiments.

III. RESULTS

A. ^{54}Fe + ^{28}Si reaction

The results of the γ-ray singles spectrum from the ^{55}Fe + ^{28}Si reaction are given in Table I. A previous study by Clements *et al.*[9] has assigned the γ rays at 96.8, 501.2, 755.6, and 962.7 keV to the decay of a positive-parity high-spin rotational band in ^{79}Rb. In that article a tenative state at 3455.1 keV which decays by an 1138.9 keV γ ray to the $(\frac{21}{2}^+)$ state at 2316.3 keV was suggested. In the ^{54}Fe + ^{28}Si reaction, ^{79}Rb was one of the strongest reaction products. The results of the γ-γ coincidence data do not show an 1138.9 keV γ ray in coincidence with the other γ rays in ^{79}Rb (see Fig. 2). However, in this experiment with the ^{54}Fe + ^{28}Si reaction we did observe an 1144.9 keV γ ray in coincidence with the other γ in ^{79}Rb (see Fig. 2). Upon measuring an angular distribution for this

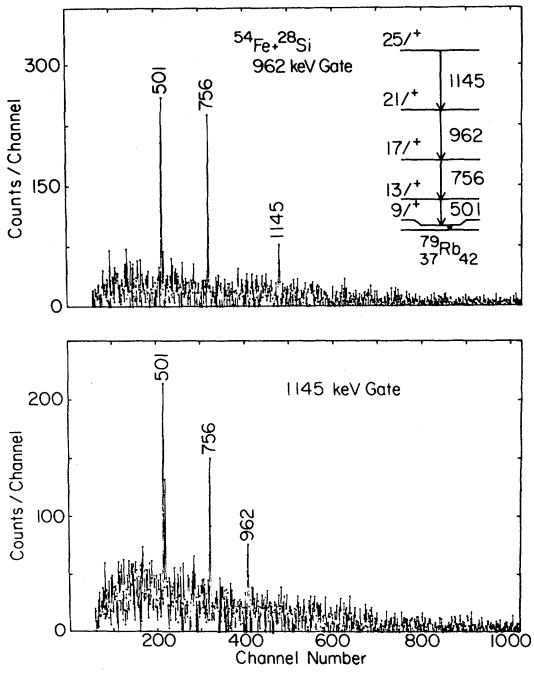

FIG. 2. γ-γ coincidence results for the reaction ^{54}Fe + ^{28}Si at E_{lab}=90 MeV. These are background-substracted spectra generated by gates on the 962 and 1145 keV γ rays in ^{79}Rb.

TABLE III. Results of angular distribution measurements for the reaction products produced in the reaction $^{54}Fe + {}^{28}Si$ at $E_{lab} = 90$ MeV.

Nucleus	E_γ (keV)	$J_i \rightarrow J_f$	A_2/A_0	A_4/A_0	X^2
^{80}Sr	386	$2^+ \rightarrow 0^+$	0.114±0.014	0.003±0.015	1.1
	596	$(4^+) \rightarrow 2^+$	0.237±0.013	0.026±0.013	0.1
	784	$(6^+) \rightarrow (4^+)$	0.266±0.008	0.025±0.008	3.8
	937	$(8^+) \rightarrow (6^+)$	0.234±0.043	−0.045±0.042	0.1
	1065	$(10^+) \rightarrow (8^+)$	0.156±0.067	0.012±0.070	0.1
^{79}Rb	501	$(\frac{13}{2}^+) \rightarrow (\frac{9}{2}^+)$	0.203±0.008	0.014±0.008	1.3
	962	$(\frac{21}{2}^+) \rightarrow (\frac{17}{2}^+)$	0.264±0.026	0.044±0.026	0.6
	1145	$(\frac{25}{2}^+) \rightarrow (\frac{21}{2}^+)$	0.162±0.057	0.001±0.058	0.1
^{76}Kr	424	$2^+ \rightarrow 0^+$	0.157±0.012	0.014±0.012	0.5
	611	$4^+ \rightarrow 2^+$	0.185±0.013	0.008±0.014	0.5
	825	$6^+ \rightarrow 4^+$	0.312±0.031	−0.007±0.030	1.5
	1019	$8^+ \rightarrow 6^+$	0.205±0.076	0.024±0.076	0.2
^{78}Kr	455	$2^+ \rightarrow 0^+$	0.116±0.025	0.017±0.026	0.2
	665	$4^+ \rightarrow 2^+$	0.194±0.035	−0.017±0.035	0.2

γ ray it was determined that the multipolarity is $E2$. Diamond *et al.*[10] and Newton *et al.*[11] have shown that $E2$ transitions in nuclei produced in these types of reactions have values of A_2/A_0 in the range of $+0.20$ to $+0.40$ and A_4/A_0 in the range of -0.04 to -0.14. The results given in Table III are consistent with these values. Therefore, we have assigned the 1144.9 keV γ ray to the decay of a level at 3461.2 keV with spin $(\frac{25}{2}^+)$ in ^{79}Rb.

Nolte *et al.*,[12] using the reaction $^{66}Zn + {}^{16}O$, have assigned the γ rays at 385.4, 594.8, and 783 keV to the decay of the 2^+, 4^+, and 6^+ levels in ^{80}Sr, respectively. With the reaction $^{54}Fe + {}^{28}Si$ these γ rays also were seen in coincidence with each other and were assigned to the decay of ^{80}Sr. In addition to the γ rays mentioned above we find that the γ rays at 937.2 and 1065.1 keV are in coincidence with the other ^{80}Sr γ rays (see Fig. 3). Also there is a possibility that an 1185.6 keV γ ray is in coincidence with these γ rays. The results of angular distribution measurements for the 937 and 1065 keV γ rays indicate that they are $E2$ type transitions (see Table III). An angular distribution for the 1186 keV γ ray was not obtained because it was too weak. From the results of these experiments we have assigned levels at 2702.2 and 3767.5 keV with spins and parities of (8^+) and (10^+), respectively, to ^{80}Sr. Also a possible level at 4953.1 keV was tentatively assigned.

Several other product nuclei were produced in the reaction $^{54}Fe + {}^{28}Si$. The gamma rays produced by the decay of these nuclei are listed in Table I along with the publications in which they were previously reported. Angular distributions for several of these gamma rays are listed in Table III. Our results are consistent with the values reported in the literature for these various nuclei.

B. $^{56}Fe + {}^{28}Si$ reaction

Prior to this investigation, the only information known about ^{81}Sr was its ground state spin and parity, $J^\pi = \frac{1}{2}^-$.[13] Recently Lister *et al.*[14] have obtained information on the β^+ decay of ^{81}Y yielding low-lying states in ^{81}Sr. From our previous studies with heavy-ion reactions of neutron-deficient nuclei in the mass $A \sim 80$ region, the $2pn$ evaporation product was known to be strongly populated. Therefore, the $^{56}Fe + {}^{28}Si$ reaction was selected as a possible reaction for studying high-spin states in ^{81}Sr. A singles spectrum from this reaction is shown in Fig. 1. The results of the singles experiment (see Table II) showed the γ rays at 772.4, 960.9, 1097.5, and 1144.6 keV to have significant strength. These γ rays had previously not been assigned to the decay of any nucleus in this mass region. An excitation function for this reaction was then taken. Results of the excitation function experiment for the above mentioned γ rays are shown in Fig. 4. These excitation functions are consistent with those resulting from the evaporation of three particles from a com-

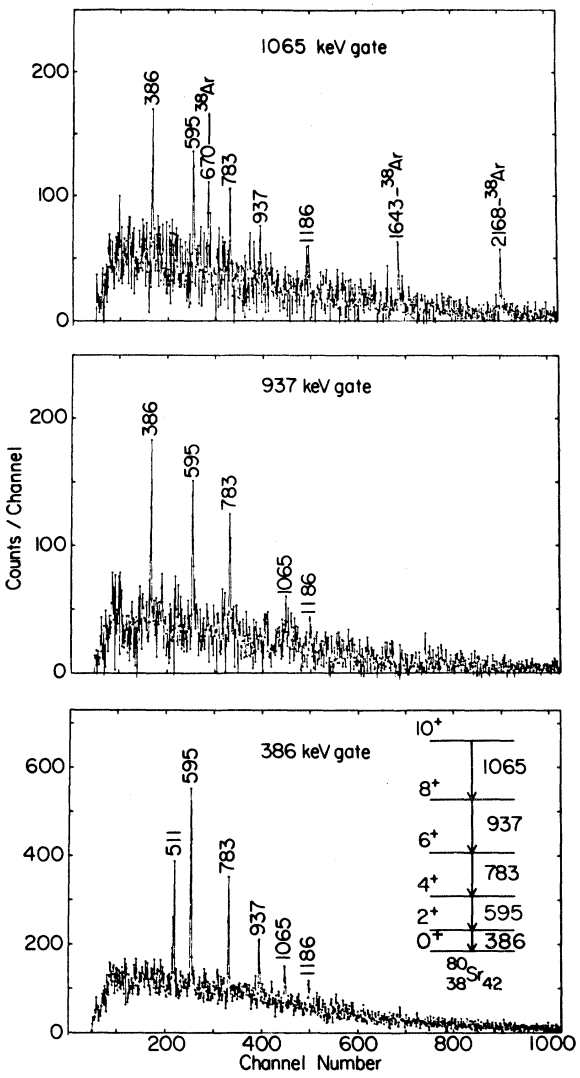

FIG. 3. γ-γ coincidence results for the reaction ^{54}Fe (^{28}Si,2$p\gamma$)^{80}Sr at $E_{lab}=90$ MeV. The background-substracted spectra shown are generated by gates on the 386, 937, and 1065 keV γ rays in ^{80}Sr.

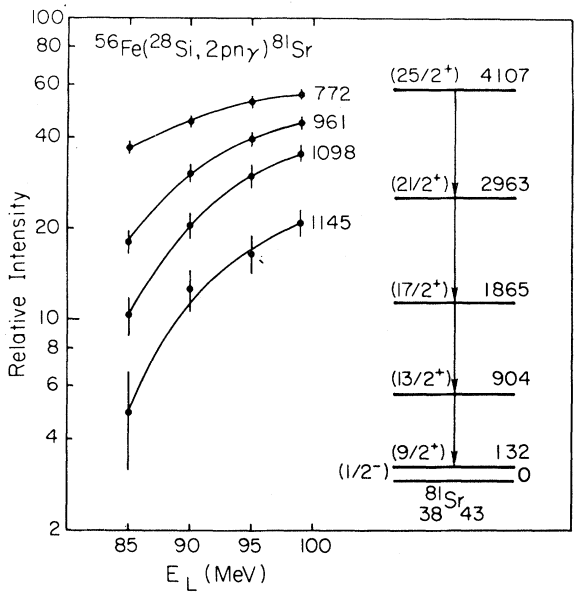

FIG. 4. Excitation functions for the γ rays assigned to the decay of ^{81}Sr from the reaction ^{56}Fe + ^{28}Si at $E_{lab}=88$ MeV. The lines are to guide the eye and the error bars represents only statistical errors.

pound nucleus[2,7] in this mass region. Also the similar slopes for the different γ rays indicate that the 772, 961, 1096, and 1145 keV γ rays may originate from the decay of the same nucleus. A γ-γ coincidence experiment was completed for the ^{56}Fe + ^{28}Si reaction at a laboratory energy of 88 MeV. The results of the γ-γ coincidence experiment are shown in Fig. 5. The gate on the 772 keV γ ray indicates that it is in coincidence with the 961, 1098, and 1145 keV γ rays. The 961 keV gate also shows it is in coincidence with the other γ rays, but in addition we see 501 and 756 keV γ rays in coincidence with the 961 keV γ ray. These γ rays have previously been assigned to the decay of ^{79}Rb and are seen here because the 962 keV γ ray in ^{79}Rb cannot be separated from the 961 keV γ ray. The 1145 keV γ ray appears with such strength because it is seen in the decay of both ^{79}Rb and ^{81}Sr. In the 1098 keV gate we again see the above mentioned γ rays, but in addition we see γ rays at 784 and 1283 keV. From a comparison of energies and the coincidence gates it has been determined that these γ rays cannot belong to the decay of the same nucleus as the 772, 961, 1098, and 1145 keV γ rays do. This indicates that two gamma rays with an energy of 1098 keV which cannot be resolved within the experimental energy resolution are produced in this reaction. At this time the γ rays at 784, 1098, and 1283 keV have not been assigned to the decay of any nucleus. Angular distribution measurements of the 772, 961, and 1098, and 1145 keV lines have been completed, the results are given in Table IV. The coefficients A_2/A_0 and A_4/A_0 are consistent with those for $E2$ transitions. The angular distributions are shown in Fig. 6.

Delayed γ spectra for the ^{56}Fe + ^{28}Si reaction were measured immediately after the beam was turned off. The spectra contain several low-lying transitions in ^{81}Rb. These transitions in ^{81}Rb result from the β^+ decay of ^{81}Sr. The strength of the

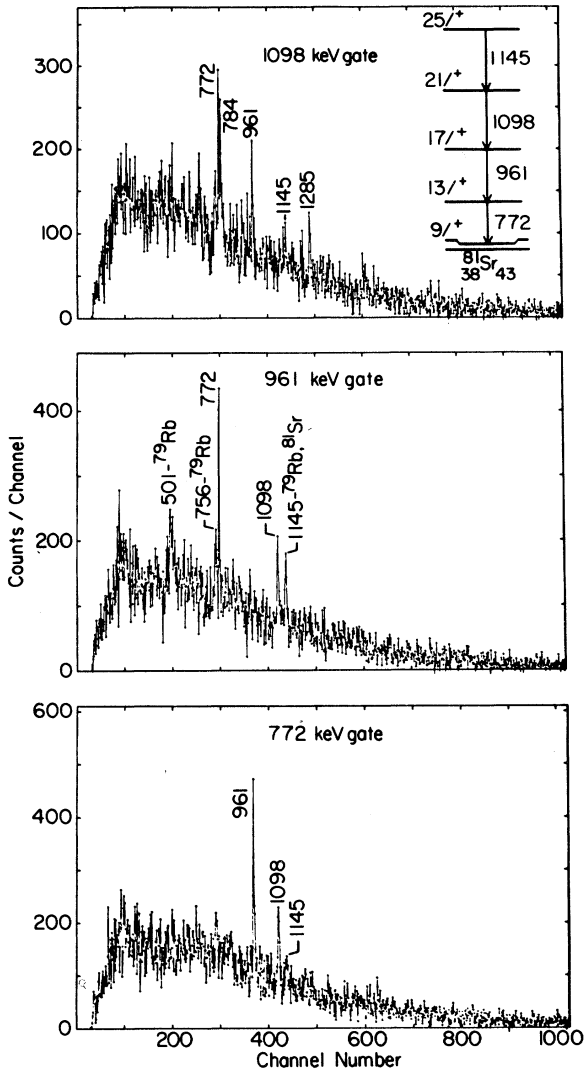

FIG. 5. γ-γ coincidence results for the reaction $^{56}Fe + ^{28}Si$ at $E_{lab}=88$ MeV. These background-subtracted spectra are generated by gates on the 772, 961, and 1098 keV γ rays assigned to the decay of ^{81}Sr.

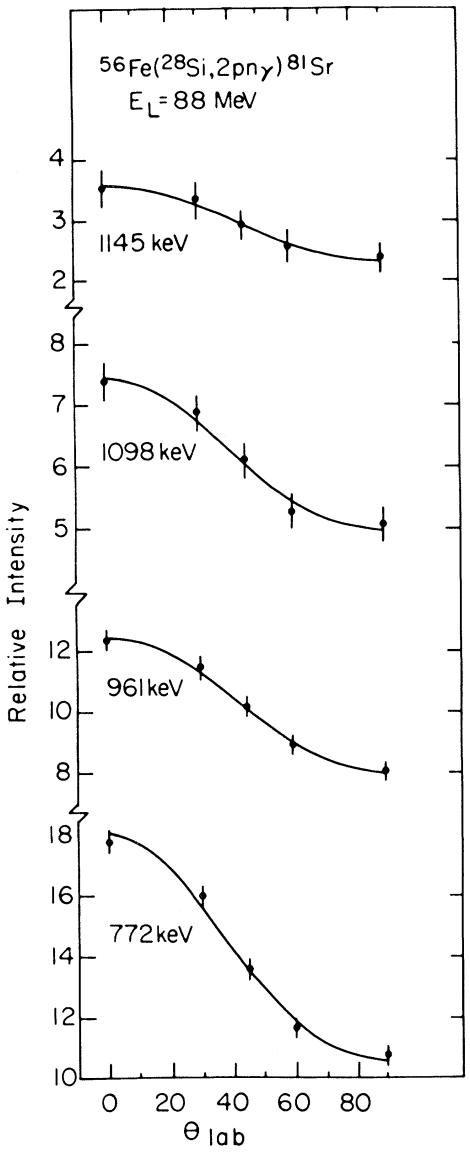

FIG. 6. Examples of angular distributions obtained from the reaction $^{56}Fe(^{28}Si,2pn\gamma)^{81}Sr$ at $E_{lab}=88$ MeV. The curves are obtained from a least squares fit to the data.

^{81}Rb γ rays in the delayed spectra suggest that ^{81}Sr is produced with significant strength in the prompt reaction. Several singles spectra (see Table V) obtained from reactions involving several different projectile and target combinations indicate that the γ rays at 772, 961, 1098, and 1145 keV are produced in the decay of ^{81}Sr. That is, in the reactions where ^{81}Sr could not be produced, they were not seen; while in those where ^{81}Sr could be produced, they were seen. Therefore, we have assigned the γ rays at 772, 961, 1098, and 1155 keV to the decay of ^{81}Sr.

The above-mentioned γ rays were assigned to a high-spin band built upon a low-lying $\frac{9}{2}^+$ level in ^{81}Sr, based upon the systematics of this mass region (see Fig. 7). Arnell *et al.*[15] have reported a level at 132 keV with a spin and parity $\frac{9}{2}^+$. Therefore, we have assigned levels at 904.4 keV with a spin and parity of $(\frac{13}{2}^+)$, 1865.3 keV with $J^\pi=(\frac{17}{2}^+)$, 2962.8 keV with $J^\pi=(\frac{21}{2}^+)$, and 4107.4 keV with

TABLE IV. Results of angular distribution measurements for the reaction products produced in the reaction $^{56}Fe + {}^{28}Si$ at $E_{lab} = 88$ MeV.

Nucleus	E_γ (keV)	$J_i \rightarrow J_f$	A_2/A_0	A_4/A_0	X^2
^{82}Sr	574	$2^+ \rightarrow 0^+$	0.245±0.023	0.023±0.024	1.4
	756	$(4^+) \rightarrow 2^+$	0.321±0.023	0.006±0.022	0.8
	901	$(6^+) \rightarrow (4^+)$	0.420±0.068	0.029±0.063	0.3
^{81}Sr	772	$(\frac{13}{2}^+) \rightarrow (\frac{9}{2}^+)$	0.367±0.024	0.054±0.023	1.7
	961	$(\frac{17}{2}^+) \rightarrow (\frac{13}{2}^+)$	0.314±0.030	0.007±0.030	0.6
	1098	$(\frac{21}{2}^+) \rightarrow (\frac{17}{2}^+)$	0.283±0.047	0.029±0.046	0.5
	1145	$(\frac{25}{2}^+) \rightarrow (\frac{21}{2}^+)$	0.295±0.094	0.006±0.092	0.2
^{81}Rb	623	$\frac{13}{2}^+ \rightarrow \frac{9}{2}^+$	0.422±0.040	0.063±0.037	1.4
	875	$\frac{17}{2}^+ \rightarrow \frac{13}{2}^+$	0.470±0.070	0.042±0.063	1.2
	1023	$\frac{21}{2}^+ \rightarrow \frac{17}{2}^+$	0.532±0.098	0.038±0.085	0.4
^{78}Kr	455	$2^+ \rightarrow 0^+$	0.298±0.019	0.014±0.018	1.2
	644	$4^+ \rightarrow 2^+$	0.337±0.030	0.066±0.029	0.9
	857	$6^+ \rightarrow 4^+$	0.280±0.042	0.012±0.042	0.4
^{79}Rb	501	$(\frac{13}{2}^+) \rightarrow (\frac{9}{2}^+)$	0.3981±0.061	−0.010±0.056	0.8

$J^\pi = (\frac{25}{2}^+)$ in ^{81}Sr. Arnell *et al.*[15] have reported a $\frac{13}{2}^+$ level at 905 keV and a $(\frac{17}{2}^+)$ level at 1866 keV, which is consistent with our results. In addition to the positive parity $K = \frac{9}{2}$ band, Arnell *et al.*[15] used the $^{78}Kr(\alpha, n\gamma)$ reaction to assign a $K = \frac{1}{2}$ positive parity band and two negative parity bands with $K = \frac{1}{2}$ and $K = \frac{5}{2}$.

As stated above the set of γ rays at 784, 1098, and 1282 were seen in coincidence with one another in the reaction $^{56}Fe + {}^{28}Si$ (see Fig. 8). This sequence of γ rays was not assigned to ^{81}Sr because the energies and the results of the coincident gates are incompatible with the level sequence assigned to ^{81}Sr. A 783.4 keV γ ray is seen in the decay of ^{39}K, a product of the contaminant reaction $^{16}O + {}^{28}Si$. However, this sequence of γ rays was not assigned to ^{39}K, because a 346.8 keV γ ray was not seen in the coincidence gates and it is in coincidence with the 783 keV γ ray in ^{39}K. Also a 783 keV γ is seen in the decay of ^{80}Sr which is produced weakly in

TABLE V. Summary of the singles measurements performed, to determine whether the γ rays indicated are from the decay of ^{81}Sr.

Reaction	Compound nucleus	E_{lab} (MeV)	γ-ray energy (keV) 772.4	960.9	1097.5	Product
$^{56}Fe + {}^{28}Si$	^{84}Zr	88	Yes	Yes	Yes	$^{81}Sr + 2pn$
$^{70}Ge + {}^{16}O$	^{86}Zr	63	Yes	Yes	No	$^{81}Sr + \alpha n$
$^{54}Fe + {}^{28}Si$	^{82}Zr	90	No[a]	No[b]	No[a]	Not possible
$^{70}Ge + {}^{14}N$	^{84}Y	63	Yes	Yes	Yes	$^{81}Sr + p2n$
$^{56}Fe + {}^{27}Al$	^{83}Y	81	Yes	Yes	Yes	$^{81}Sr + pn$
$^{54}Fe + {}^{27}Al$	^{81}Y	81	No	No[b]	No	Not possible
$^{68}Zn + {}^{16}O$	^{84}Sr	63	Yes	No	No	$^{81}Sr + 3n$
$^{64}Zn + {}^{16}O$	^{80}Sr	56	No	No	No	Not possible
$^{70}Ge + {}^{12}C$	^{82}Sr	47	Yes[c]	No	No	$^{81}Sr + 1n$

[a]771.6 and 1098.6 keV γ rays were observed weakly and not assigned to any reaction product from this reaction. These γ rays, however, were not seen in coincidence with each other though. This indicates that these γ rays are not the same γ rays as those observed in the $^{56}Fe + {}^{28}Si$ reaction.

[b]A 962.4 keV γ ray was observed in this reaction, but it was assigned to ^{79}Rb.

[c]Assigned to the decay of ^{76}Se.

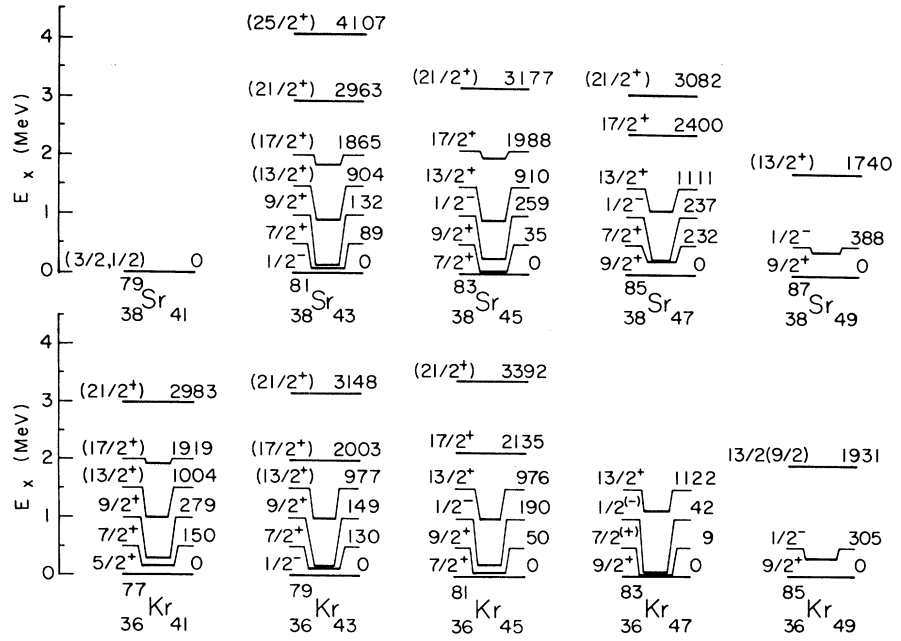

FIG. 7. Systematics of the neutron-deficient odd-mass Kr and Sr isotopes. Note the similarities of the spins and excitation energies for the low-lying states between the Kr and Sr isotopes with same number of neutrons.

this reaction. This sequence of γ rays was not assigned to ^{80}Sr because they were not seen in coincidence with the other γ rays from the decay of ^{80}Sr, in the reaction ^{54}Fe + ^{28}Si which produces ^{80}Sr very strongly.

Compound nuclear evaporation model calculations were completed and indicate ^{80}Rb should be produced. However, the 784 and 1098 keV γ rays were seen in the ^{54}Fe + ^{28}Si reaction in which ^{80}Rb cannot be produced. This does not eliminate ^{80}Rb as a possibility, since these γ rays could be from a different product in the ^{54}Fe + ^{28}Si reaction. For example, in the ^{54}Fe + ^{28}Si reaction the 784 keV γ ray is produced by the decay of both ^{80}Sr and ^{39}K. Several other singles measurements were made, but these measurements also do not eliminate or confirm ^{80}Rb as a candidate nucleus for the assignment of these γ rays. Therefore, we have not assigned the sequence of γ rays at 784, 1098, and 1283 keV to the decay of any nucleus.

The reaction ^{56}Fe + ^{28}Si produced several other nuclei, in addition to ^{81}Sr. The energies of the gamma rays produced in the decay of these nuclei are listed in Table II along with the publications in which they were previously reported. The results of angular distribution measurements on some of these gamma rays are given in Table IV. In all cases our results agree with those reported in the literature for these nuclei.

IV. DISCUSSION

A. ^{79}Rb

As mentioned above, the reaction ^{54}Fe + ^{28}Si was used to investigate high-spin states in ^{79}Rb. Clements *et al.*[9] showed that the ground state positive-parity high-spin band in ^{79}Sb is based upon a low-lying $1g_{9/2}$ proton single particle state. Friedrichs *et al.*[16] showed that positive-parity bands in the mass $A \sim 80$ region can be described in terms of the rotation aligned coupling (RAC) model of Stephens *et al.*[17] In this model the Coriolis interaction weakens the coupling between the odd particle and the rotating even-even core, in which case the rotation axes of the odd particle and the core become aligned. The result is that the rotation has little effect on the coupling of the particle to the core

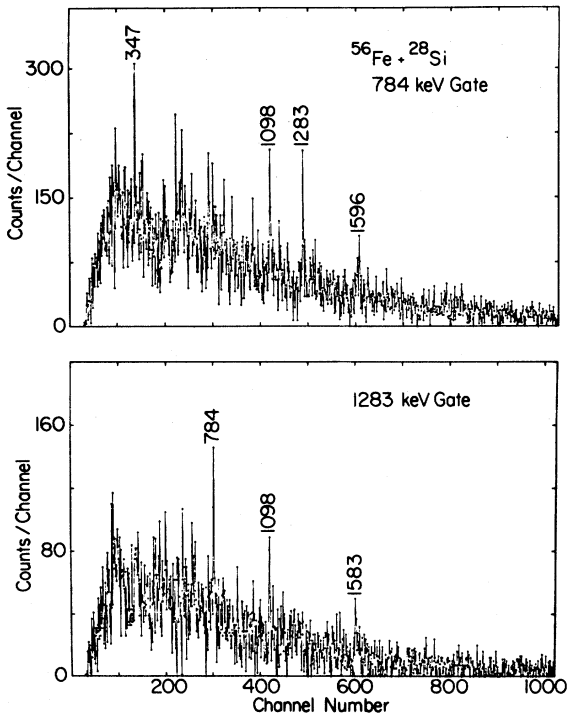

FIG. 8. γ-γ coincidence results for the unassigned sequence of γ rays in the reaction ^{56}Fe + ^{28}Si at E_{lab} = 88 MeV. These are background-subtracted gated spectra.

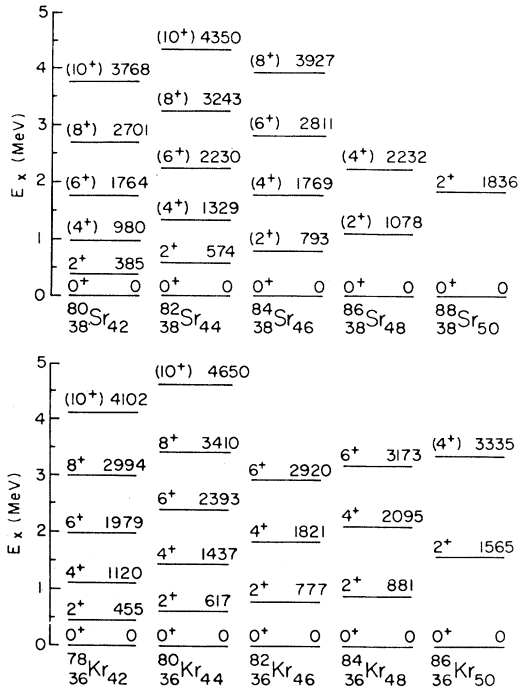

FIG. 10. Systematics of the neutron-deficient even-even Kr and Sr isotopes. Note the compression of level energies for a given spin as the isotopes become more neutron deficient.

and the bands are referred to as "rotation-particle decoupled" bands. These bands are characterized by the levels decaying by $E2$ transitions and the energy spacings of the band being very similar to the ground state band energy spacings of the even-even core.[16,17] The positive parity band in ^{79}Rb fits very well with this type of description as is shown in Fig. 9, as well as the new level at 3461.2 keV with $J^{\pi}=(\frac{25}{2}^{+})$ in ^{79}Rb.

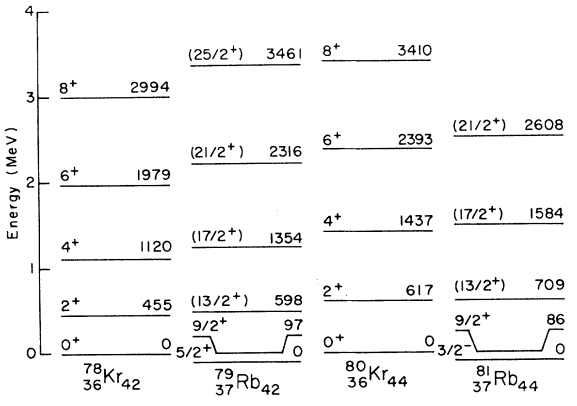

FIG. 9. Comparison of the positive-parity band in ^{79}Rb with the ground state band in ^{78}Kr and the ^{80}Kr and ^{81}Rb levels (Ref. 9).

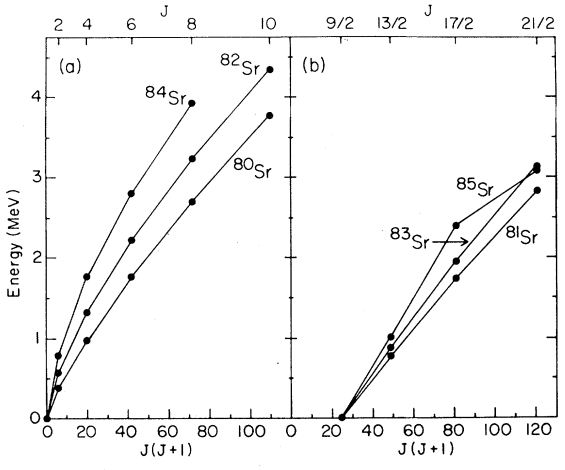

FIG. 11. Graph of the energy levels as a function of $J(J+1)$ for Sr isotopes. (a) $J(J+1)$ plot for even-even neutron-deficient Sr nuclei. (b) $J(J+1)$ for odd-mass neutron-deficient Sr nuclei.

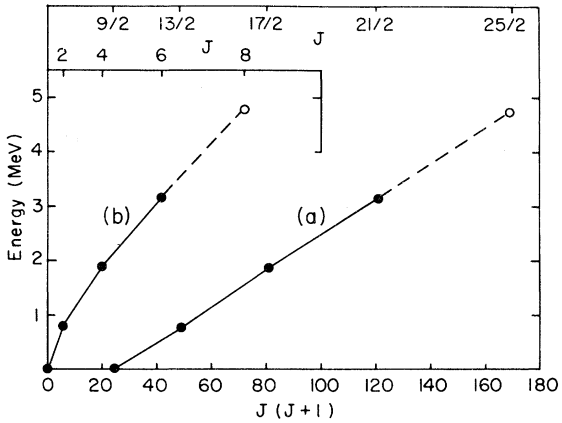

FIG. 12. Graph of the energy levels versus $J(J+1)$ for the sequence of unassigned gamma rays. (a) $J(J+1)$ plot of the sequence if it were built upon a low-lying $\frac{9}{2}$ level. This is the result for an odd-mass nucleus with $A \sim 80$. (b) A $J(J+1)$ plot for the sequence of levels if it belongs to an even-even nucleus. Note these graphs are similar to the graphs seen in Fig. 10.

B. ^{80}Sr

The reaction ^{54}Fe + ^{28}Si was also used to study high-spin states in ^{80}Sr. The new levels at 2702.2 and 3767.5 keV with $J^{\pi}=(8^{+})$ and (10^{+}), respectively, fit quite well into the systematics of this mass region, as is shown in Fig. 10. That is, the energy levels for a given spin decrease systematically as the isotopes become more neutron deficient. Now, we wish to compare the high-spin positive parity sequence with that of a rotational nucleus. To make this comparison we plot the energy levels as a function of $J(J+1)$ as is shown in Fig. 11(a). In such a plot the spectrum of a rigid rotor is represented by a straight line. As is seen in Fig. 11, the yrast states in the even Sr isotopes are qualitatively described by the rigid rotor. Also it is seen that as the isotopes become more neutron deficient they become more deformed, since the moment of inertia (I) is a measure of the deformation of a rotational nucleus.

C. ^{81}Sr

The reaction ^{56}Fe + ^{28}Si was used to assign a positive parity high-spin level sequence in ^{81}Sr, up to the $(\frac{25}{2}^{+})$ state. We have plotted the energy levels of the odd Sr isotopes as a function of $J(J+1)$ to investigate their rotational characteristics in Fig. 11(b). Again we see that as the isotopes become more neutron deficient they become more deformed, as would be expected since the isotoptes are getting further away from the closed neutron shell at $N=50$.

D. Other γ transitions

As stated above the sequence of γ rays at 784, 1098, and 1283 keV seen in the reaction ^{56}Fe + ^{28}Si, were not assigned to the decay of any nucleus. Figure 12 shows a graph of this sequence of energy levels as a function $J(J+1)$. The curve labeled "a" in Fig. 12 is a $J(J+1)$ plot of the level sequence as if it were built on a low-lying $\frac{9}{2}^{+}$ level. The curve labeled "b" is a $J(J+1)$ plot of the level sequence for an even-even nucleus. The results of these graphs show that this sequence of levels is consistent with the systematics in this mass region for a deformed rotational band built on a low-lying $\frac{9}{2}^{+}$ state or that of an even-even nucleus.

V. CONCLUSIONS

The ^{28}Si + ^{54,56}Fe reactions have proved to be very useful in studying high-spin states in neutron deficient nuclei in the $A \approx 80$ region. New states have been observed in ^{79}Rb, ^{80}Sr, and ^{81}Sr. Another sequence of levels has been found which has not yet been assigned to any nucleus. The new levels are consistent with and extend the systematics of the quasirotational bands in this mass range. There is a steady increase in the moment of inertia of both the even and odd mass Kr and Sr isotopes as the neutron number decreases from the shell closure at $N=50$. Such systematic behavior suggests that much can be learned about the interplay of collective and single-particle degrees of freedom from further study in the $A \approx 80$ region.

ACKNOWLEDGMENTS

The authors wish to thank Bob Leonard for preparing the Fe targets. This work was supported in part by the National Science Foundation.

*Permanent address: Bell Laboratories, Holmdel, New Jersey 07733.

†Permanent address: Division of Science and Mathematics, Fordham University, New York, New York 10023.

[1]L. R. Medsker, D. C. Wilson, and L. H. Fry, Jr., Phys. Lett. 74B, 39 (1978).

[2]L. R. Medsker, L. V. Theisen, L. H. Fry, Jr., and J. S. Clements, Phys. Rev. C 19, 790 (1979).

[3]K. R. Chapman, Nucl. Instrum. Methods 124, 229 (1975).

[4]Mixed radionuclide standard (4215E) from the National Bureau of Standards.

[5]The code PEAKFIT courtesy of P. P. Singh, Indiana University Cyclotron Facility. Modified by R. V. LeClaire for interactive scope use at Florida State University.

[6]The code ANGDIS, written by J. S. Clements, Florida State University (unpublished).

[7]P. Taras and B. Haas, Nucl. Instrum. Methods 123, 73 (1975).

[8]The code RAMPS, written by R. V. LeClaire, Florida State University (unpublished).

[9]J. S. Clements, L. R. Medsker, L. H. Fry, Jr., L. V. Theisen, and L. A. Parks, Phys. Rev. C 20, 164 (1979).

[10]R. M. Diamond, E. Matthais, J. O. Newton, and F. S. Stephens, Phys. Rev. Lett. 16, 1205 (1966).

[11]J. O. Newton, F. S. Stephens, R. M. Diamond, K. Kotajima, and E. Matthais, Nucl. Phys. A95, 357 (1967).

[12]E. Nolte, Y. Shida, W. Kutschera, R. Prestele, and H. Morinaga, Z. Phys. 268, 267 (1974).

[13]R. Broda, A. Z. Zrynkiewicz, J. Stycén and W. Walus, Nucl. Phys. A216, 493 (1973).

[14]C. J. Lister, P. E. Haustein, D. E. Alburger, and J. W. Olness, Phys. Rev. C 24, 260 (1981).

[15]S. E. Arnell, Ö. Skeppstedt, E. Wallander, and A. Nilsson, Inst. Phys. Conf. Ser. 49, 240 (1979).

[16]H. G. Friderichs, A. Gelberg, B. Heits, K. O. Zell, and P. von Brentano, Phys. Rev. C 13, 2247 (1976).

[17]F. S. Stephens, R. M. Diamond, J. R. Leigh, T. Kammuri, and K. Nakai, Phys. Rev. Lett. 29, 438 (1972).

[18]Y. A. Ellis, Nucl. Data Sheets V9, 319 (1972).

[19]M. A. Van Driel, H. H. Eggenhuisen, G. A. P. Engelbertink, L. P. Ekström, and J. A. J. Hermans, Nucl. Phys. A272, 466 (1976).

[20]M. Uhrmacher, J. Dauk, N. Wüst, K. P. Lieb, and A. M. Kleinfeld, Z. Phys. A 272, 403 (1975).

[21]H. H. Eggenhuisen, L. P. Ekström, G. A. P. Engelbertink, H. J. M. Aarts, and G. J. Langevield, Nucl. Phys. A299, 175 (1978).

[22]R. L. Robinson, H. J. Kim, J. B. McGrory, G. J. Smith, W. T. Milner, R. O. Sayer, J. C. Wells, Jr., and J. Lin, Phys. Rev. C 13, 1922 (1976).

[23]J. Liptak and J. Kristiak, Nucl. Phys. A311, 421 (1978).

[24]F. E. Bertrand and R. L. Auble, Nucl. Data Sheets V19, 507 (1976).

[25]J. S. Clements, L. R. Medsker, L. H. Fry, Jr., and L. V. Theisen, Phys. Rev. C 21, 1285 (1980).

[26]E. Nolte and P. Vogt, Z. Phys. A 275, 33 (1975).

[27]H. Morinaga and T. Yamazaki, *In-Beam Gamma-Ray Spectroscopy* (North-Holland, Amsterdam, 1976), p. 11.

[28]J. F. Lemming, Nucl. Data Sheets V15, 137 (1975).

[29]P. P. Urone and F. E. Bertrand, Nucl. Data Sheets V15, 107 (1975).

[30]H. G. Friederichs, A. Gelberg, B. Heits, K. O. Zell, and P. Von Brentano, Phys. Rev. C 13, 2247 (1976).

[31]A. Dewald, W. Gast, A. Gelberg, K. Neuenhofer, K. O. Zell, and P. von Brentano, private communication.